Z. Phys. A – Atomic Nuclei 333, 299–306 (1989)

Zeitschrift für Physik A
Atomic Nuclei

Nonstatistical Structures in the Excitation Functions of $^{20}Ne(^{16}O, ^{12}C)^{24}Mg$ and $^{20}Ne(^{16}O, ^{20}Ne)^{16}O$ Reactions

A. Sarma and R. Singh
Physics Department, North-Eastern Hill University, Shillong, India

Received November 2, 1988; revised version March 8, 1989

The data on the excitation functions of $^{20}Ne(^{16}O, ^{12}C)^{24}Mg$, $^{20}Ne(^{16}O, ^{12}C)\,^{24}Mg^*(1.37, 2^+)$, $^{20}Ne(^{16}O, ^{12}C)\,^{24}Mg^*(4.12, 4^+ + 4.24, 2^+) + ^{20}Ne(^{16}O, ^{12}C^*(4.44, 2^+))\,^{24}Mg$, $^{20}Ne(^{16}O, ^{12}C)\,^{24}Mg^*(6.01, 4^+ + 6.43, 0^+)$, $^{20}Ne(^{16}O, ^{20}Ne)\,^{16}O$, $^{20}Ne(^{16}O, ^{20}Ne^*(1.63, 2^+))\,^{16}O$, and $^{20}Ne(^{16}O, ^{20}Ne^*(4.25, 4^+))\,^{16}O$ reactions at $\theta_{lab} = 13°$ from $E_{c.m.} = 22.8$ to 38.6 MeV have been subjected to a statistical analysis comprising of the calculations of the distribution of cross sections, deviation functions, cross-correlation functions, summed excitation functions, cross-channel correlation coefficients and coherence widths. The analysis confirms the existence of nonstatistical structures at $E_{c.m.} = 24.6$, 27.8, 31.7 and 35.5 MeV, and identifies a new structure of the same nature at $E_{c.m.} = 25.6$ MeV.

PACS: 24.60. Dr; 25.70. Ef; 25.70 – Z

1. Introduction

Intermediate structure [1] as well as statistical fluctuations [2, 3] have been reported in the excitation functions of elastic and inelastic scattering of $^{12}C + ^{24}Mg$. Intermediate structure has also been observed in strongly damped $^{12}C + ^{24}Mg$ reactions of orbiting type. In fact, the observation of large ($\sim$250 to 460 keV) coherence widths provides evidence for a long lived intermediate dinuclear type of configuration [4]. In $A = 36$ system resonances have been observed through the studies of $^{24}Mg(^{12}C, ^4He)^{32}S$ reaction [5], and of $^{24}Mg + ^{12}C$ and $^{16}O + ^{20}Ne$ elastic and inelastic scattering [6, 7]. A recent experimental investigation [8] of $^{20}Ne(^{16}O, ^{12}C)^{24}Mg$ and $^{20}Ne(^{16}O, ^{20}Ne)^{16}O$ reactions between $E_{c.m.} = 22.8$ and 38.6 MeV showed that there were resonant structures at $E_{c.m.} = 24.5$, 27.8, 31.7 and 35.5 MeV with their J-values ranging from 18 to 25 $\hbar$. These spins were, of course, determined by comparing the experimental angular distributions of the ground-state transition of $^{20}Ne(^{16}O, ^{12}C)^{24}Mg$ reaction, measured at the bombarding energies corresponding to the correlated maxima in the excitation functions, with $P_J^2(\cos\theta)$ shapes. The reported resonant structures seem to be characterised by grazing angular momenta values of the $^{12}C + ^{24}Mg$ channel. The same inference was drawn through a study of $^{24}Mg(^{12}C, ^4He)^{32}S$ reaction [5]. However, the grazing angular momenta in the $^{16}O + ^{20}Ne$ channel were found to be two or more units larger than the J-values deduced from the angular distributions (mentioned above).

The resonant structures in $^{20}Ne(^{16}O, ^{12}C)^{24}Mg$ and $^{20}Ne(^{16}O, ^{20}Ne)^{16}O$ excitation functions were located by calculating the corresponding deviation functions [8]. From the analysis of the data the authors obtained a value of $\geqq 0.95$ for the fraction of cross section contributed by direct reaction (non-compound) by assuming the number of effective channels to be one [8]. This assumption need not necessarily be good [9], specially noting the fact that the angle of observation is much different from zero degree. The cross-correlation coefficients were found to be positive. Thus essentially the analysis of these data was limited to the calculations of cross correlation coefficients (which were not given in the paper), the deviation functions, and the probability limits for finding deviations larger than 0.2. In order to ascertain the origin of the observed structures in the excitation functions of $^{20}Ne(^{16}O, ^{12}C)^{24}Mg$ and $^{20}Ne(^{16}O, ^{20}Ne)^{16}O$ reactions we have carried out a much more detailed statistical analysis of these data following the

approach of Ericson [10], and Brink and Stephen [11]. The present analysis consists of the calculations of the Hauser-Feshbach cross sections, number of effective channels, the distribution of cross sections, energy dependent cross-correlation functions, deviation functions, cross-channel correlation coefficients, and coherence widths. Such an analysis is expected to provide a quantitative estimate of the likelihood that the observed structures are of statistical origin or they arise from some nonstatistical mechanism.

2. Analysis

2.1. Data Reduction

The data on the excitation functions of $^{20}Ne(^{16}O, ^{12}C)^{24}Mg$ and $^{20}Ne(^{16}O, ^{20}Ne)^{16}O$ reactions were taken from [8]. Since we want to compare the behaviour of the experimental cross sections with the predictions of the statistical model, the energy dependent gross structure should be removed from the excitation functions. This was done by following the approach of Pappalardo [12] according to which the experimental cross sections, $d\sigma(E)$, are divided by the running average, $\langle d\sigma(E)\rangle$ taken over a suitable energy interval, $\Delta E_{c.m.}$. The criterion that is usually followed for choosing $\Delta E_{c.m.}$ is $\Gamma_{fine} \ll \Delta E_{c.m.} \ll \Gamma_{gross}$, where Γ_{fine} and Γ_{gross} indicate the respective fine and gross structure widths observed in the excitation function [13]. However, if the value of $C(0)$, the normalised variance of the reduced excitation function, $(C(0)=\langle x^2\rangle/\langle x\rangle^2 - 1;\ x=d\sigma(E)/\langle d\sigma(E)\rangle)$ is plotted as a function of averaging interval, $\Delta E_{c.m.}$, a plateau is expected to be obtained when $\Delta E_{c.m.}$ very well exceeds the coherence width [14]. The appropriate value of $\Delta E_{c.m.}$ can, therefore, be taken from such plots. The variation of $C(0)$ with $\Delta E_{c.m.}$ for all the seven excitation functions is shown in Fig. 1. Noting the behaviour of $C(0)$ with $\Delta E_{c.m.}$ and the widths, Γ_{fine} and Γ_{gross}, we chose $\Delta E_{c.m.} = 2.0$ MeV for data reduction. It might be mentioned that Schimizu et al. [8] took an averaging interval of 2.2 MeV for this purpose. It was this trend reduced data that was subjected to the analysis.

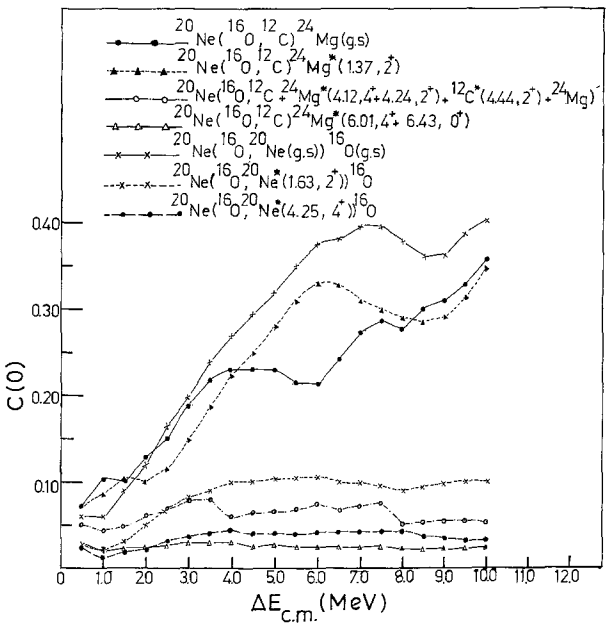

Fig. 1. Variation of the variance $C(0)$, with the variation of averaging interval $\Delta E_{c.m.}$, (in MeV) for the indicated excitation functions of $^{20}Ne(^{16}O, ^{12}C)^{24}Mg$ and $^{20}Ne(^{16}O, ^{20}Ne)^{16}O$ reactions

2.2. Hauser-Feshbach Cross Sections and Number of Effective Channels

The theoretical cross sections for $^{20}Ne(^{16}O, ^{12}C)^{24}Mg$, $^{20}Ne(^{16}O, ^{12}C)^{24}Mg^*(1.37, 2^+)$, and $^{20}Ne(^{16}O, ^{12}C)^{24}Mg^*(4.12, 4^+ + 4.24, 2^+)$ reactions were calculated by the statistical model code STATIS [15] which employs the Hauser-Feshbach expression [16] for evaluating energy averaged differential cross sections for populating the specific final states. The $n+^{35}Ar$, $p+^{35}Cl$, $^4He+^{32}S$, $^8Be+^{28}Si$ and $^{12}C+^{24}Mg$ exit channels were included in the calculation. The required transmission coefficients for these calculations were obtained by using the optical model code HOP2 [17]. The optical model and level density parameters for these calculations were taken from the literature [9, 18]. The theoretical and experimental cross sections are shown in Fig. 2. Here it should be noted that the experimental cross sections for $^{20}Ne(^{16}O, ^{12}C)^{24}Mg^*(4.12, 4^+ + 4.24, 2^+)$ have contributions from $^{20}Ne(^{16}O, ^{12}C^*(4.44, 2^+))^{24}Mg$ process also, whereas the theoretical cross sections do not. From this figure it can be noted that the theoretical cross sections are upto much more than an order of magnitude smaller than the experimental ones. This already shows that major part of the cross section results from contribution of non-compound processes prevailing in the reaction. A similar behaviour is expected for the other excitation functions. We shall come back to this point later.

The code STATIS [15] was also used to calculate the number of effective channels N, the quantity that determines the statistically independent cross sections which contribute to the measured cross sections. This number is of crucial importance for the calculation of the theoretical distributions of cross sections (see next section). The details of evaluation of N are given in [15] and [19]. The variation of N with angle for $^{20}Ne(^{16}O, ^{12}C)^{24}Mg$, $^{20}Ne(^{16}O, ^{12}C)^{24}Mg^*(1.37, 2^+)$ and $^{20}Ne(^{16}O, ^{12}C)^{24}Mg^*(4.12, 4^+ + 4.24, 2^+)$ excita-

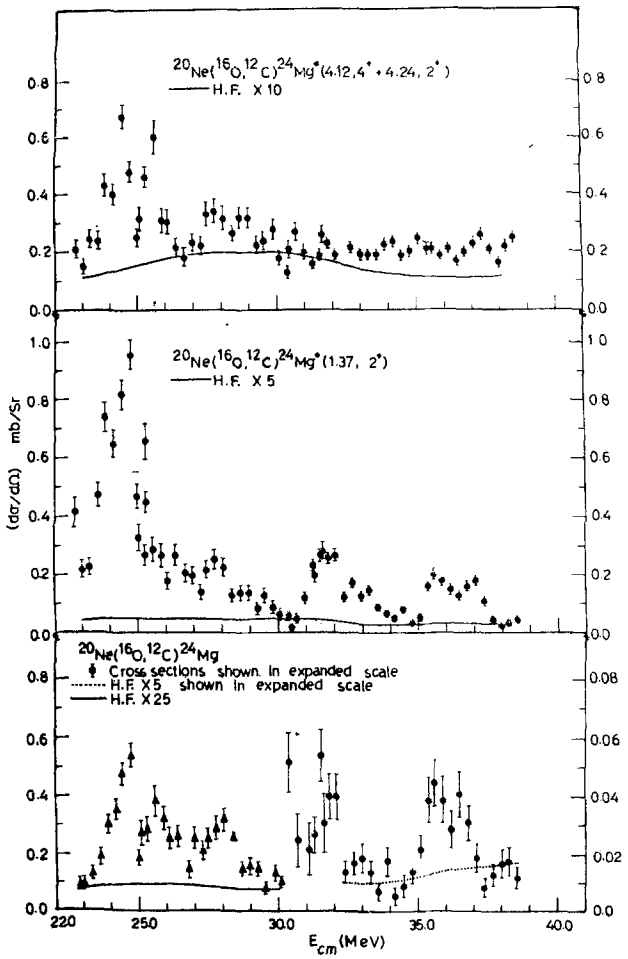

Fig. 2. Comparison of experimental and theoretical (Hauser-Feshbach) cross sections for the indicated excitation functions of $^{20}Ne(^{16}O, ^{12}C)^{24}Mg$ reaction (see text)

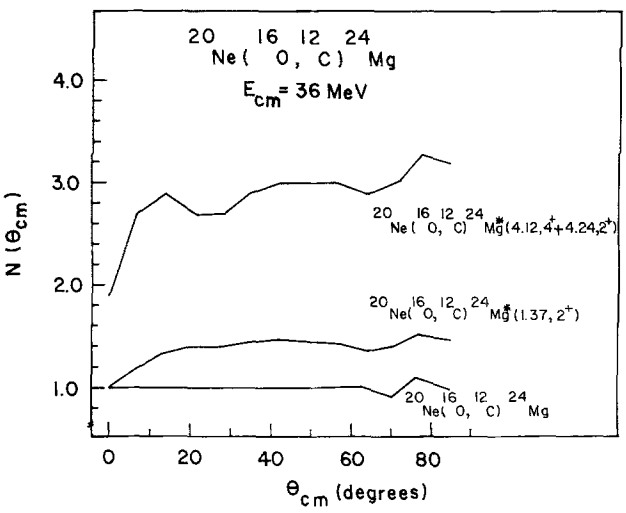

Fig. 3. Variation of the number of effective channels, N, with angle, $\theta_{c.m.}$, at $E_{c.m.}=36$ MeV for the indicated excitation functions of $^{20}Ne(^{16}O, ^{12}C)^{24}Mg$ reaction

Table 1. The calculated values of N at $\theta_{c.m.}=21°$ for the three excitation functions at $E_{c.m.}=23$ and 38 MeV

$E_{c.m.}=23.00$ MeV Exit-channel (excitation function)	Value of N
1. $^{12}C+^{24}Mg$	1.00
2. $^{12}C+^{24}Mg^*(1.37, 2^+)$	1.52
3. $^{12}C+^{24}Mg^*(4.12, 4^+ + 4.24, 2^+)$	2.50
$E_{c.m.}=38.00$ MeV Exit-Channel (excitation function)	Value of N
1. $^{12}C+^{24}Mg$	1.00
2. $^{12}C+^{24}Mg^*$ (1.37, 2^+)	1.34
3. $^{12}C+^{24}Mg^*$ (4.12, $4^+ + 4.24, 2^+$)	2.80

tion functions is shown in Fig. 3. The values of N at $\theta_{c.m.}\approx 21°$ (corresponding to $\theta_{lab}=13°$ at which the measurements were made) at $E_{c.m.}=23$ and 38 MeV for the above mentioned exit channels are given in Table 1. Thus, as expected, except for the ground state transition, the values of N exceed unity, obviously contrary to the assumption made by Schimizu et al. [8] for obtaining the probability distributions.

2.3. *Distributions of Cross Sections*

In presence of direct reactions, the distribution of fluctuating cross sections is given by [11, 19]

$$P(x)=\left(\frac{N}{1-Y_d}\right)^N x^{N-1}\exp\left(-N\frac{x+Y_d}{1-Y_d}\right)\cdot\frac{I_{N-1}[2N\sqrt{xY_d}/(1-Y_d)]}{[N\sqrt{xY_d}/(1-Y_d)]^{N-1}} \quad (1)$$

where, as mentioned earlier, $x=d\sigma(E)/\langle d\sigma(E)\rangle$, N the number of effective channels, Y_d the ratio of the average direct (non-compound) to total cross section, and I_{N-1} is the modified Bessel function of order $N-1$. The quantities N and Y_d are related to each other via the relation [14]

$$C(0)=\frac{1-Y_d^2}{N} \quad (2)$$

where $C(0)$ is the variance of the data, as mentioned earlier. Thus knowing $C(0)$ and N, Y_d can be obtained from (2). The value of Y_d can also be estimated from the relation

$$Y_d=\left\langle\frac{\langle d\sigma(E)\rangle - d\sigma\ \text{H.F.}}{\langle d\sigma(E)\rangle}\right\rangle \quad (3)$$

where $d\sigma$ H.F. is the calculated Hauser-Feshbach cross section and $\langle d\sigma(E)\rangle$, the average experimental cross section. The symbol $\langle\ \rangle$ denotes the average

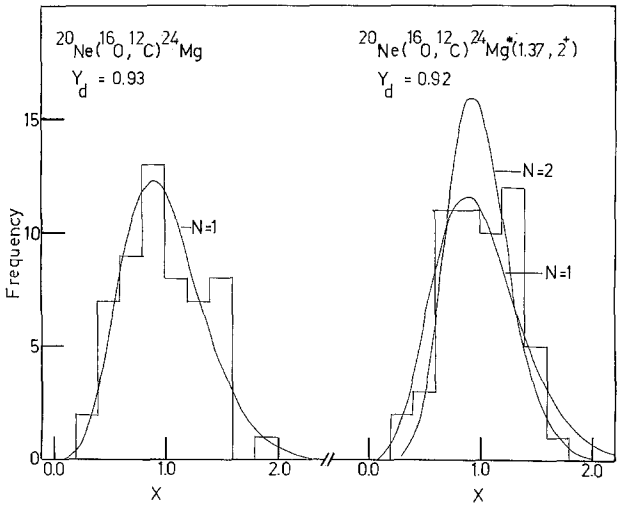

Fig. 4. Experimental (histograms) and theoretical (continuous curves) distributions of cross sections for the indicated excitation functions of $^{20}Ne(^{16}O, ^{12}C)^{24}Mg$ reaction. The appropriate values of Y_d and N have been indicated

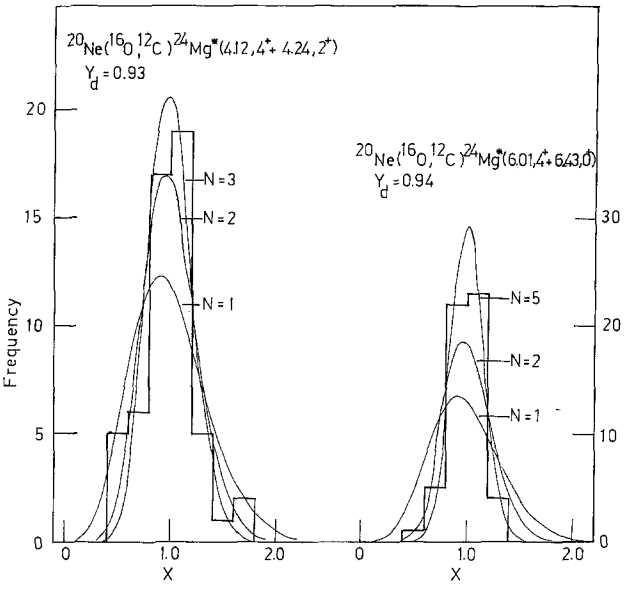

Fig. 5. Same as in Fig. 4 but for the indicated excitation functions of $^{20}Ne(^{16}O, ^{12}C)^{24}Mg$ reaction. Theoretical distributions for $N=1$ are shown for comparison

taken over the entire energy range. We estimated the values of Y_d by using both (2), and (3) (for the excitation functions corresponding to which the Hauser-Feshbach cross sections were calculated). The values of Y_d thus obtained agreed very well with each other, and turned out to be somewhat lower than the ones ($Y_d \geqq 0.95$) mentioned by Schimizu et al. [8]. These authors obtained larger values of Y_d simply because they took $N=1$ for all the excitation functions.

For $^{20}Ne(^{16}O, ^{12}C)^{24}Mg$ reaction the experimental (histogram) and theoretical distributions have been compared in Figs. 4 and 5. For $^{12}C+^{24}Mg$ exit channel, $N=1$ but for $^{12}C+^{24}Mg^*(1.37, 2^+)$ channel it is about 1.4. Therefore, for the latter the theoretical distributions have been calculated for $N=1$ and 2 both (see Fig. 4). Good agreement between experimental and theoretical distributions (Fig. 4) indicates a large non-statistical component [21] in the cross sections. For $^{12}C+^{24}Mg^*(4.12, 4^+ + 4.24, 2^+)$ channel the calculated value of N lies between 2 and 3, and therefore, we calculated the theoretical distributions for both these values of N. Here again, there is quite a good agreement between experimental and theoretical distributions, as can be noted from Fig. 5. This also points to a large non-statistical component in the cross section. It might, however, be kept in mind that in the experimental distribution there are contributions from $^{12}C^*(4.44, 2^+)+^{24}Mg$ channel also.

The values of N were not theoretically calculated for $^{12}C+^{24}Mg^*(6.01, 4^+ + 6.43, 0^+)$ channel. However, noting the value of N for $^{12}C+^{24}Mg^*(4.12, 4^+ + 4.24, 2^+)$ channel we calculated the theoretical distribution of cross section for $^{12}C+^{24}Mg^*(6.01, 4^+ + 6.43, 0^+)$ channel for $N=2$ as well as for $N = N_{max}(=5)$ given by [10]

$$N_{max} = g/2 \quad \text{(for even } g\text{)}$$
$$= (g+1)/2 \quad \text{(for odd } g\text{)} \qquad (4)$$

with $g=(2i+1)(2I+1)(2i'+1)(2I'+1)$
where i and I are the the spins of the projectile and target and i' and I' are the spins of the final fragments respectively. The value of Y_d was obtained by using $N=2$ and the appropriate value of $C(0)$. The experimental and theoretical distributions are shown in Fig. 5 from where good agreement between the two can be noted. This comparison also indicates large non-statistical component in the cross sections. This fact (the dominance of non-statistical process) was already indicated by the comparison of experimental and theoretical (Hauser-Feshbach) cross sections for first three $^{12}C+^{24}Mg$ exit channels (see Sect. 2.2).

For $^{20}Ne(^{16}O, ^{20}Ne)^{16}O$ excitation function the value of N is unity. The experimental and theoretical distributions for the same are given in Fig. 6a. Here also a large non-statistical component in the cross sections is clearly reflected. Since we did not do the theoretical calculations for N for $^{20}Ne^*(1.63, 2^+) + ^{16}O$, and $^{20}Ne^*(4.25, 4^+)+^{16}O$ exit channels, we used $Y_d=0.92$ and 0.94 respectively, same as for $^{12}C + ^{24}Mg^*(1.37, 2^+)$, and $^{12}C+^{24}Mg^*(6.01, 4^+ + 6.43, 0^+)$, for calculating the theoretical distributions. For $^{20}Ne^*(1.63, 2^+)+^{16}O$ channel theoretical distributions have been calculated for $N=1$ and 2 both (like for $^{12}C+^{24}Mg^*(1.37, 2+)$) as well as for $N_{max}=3$,

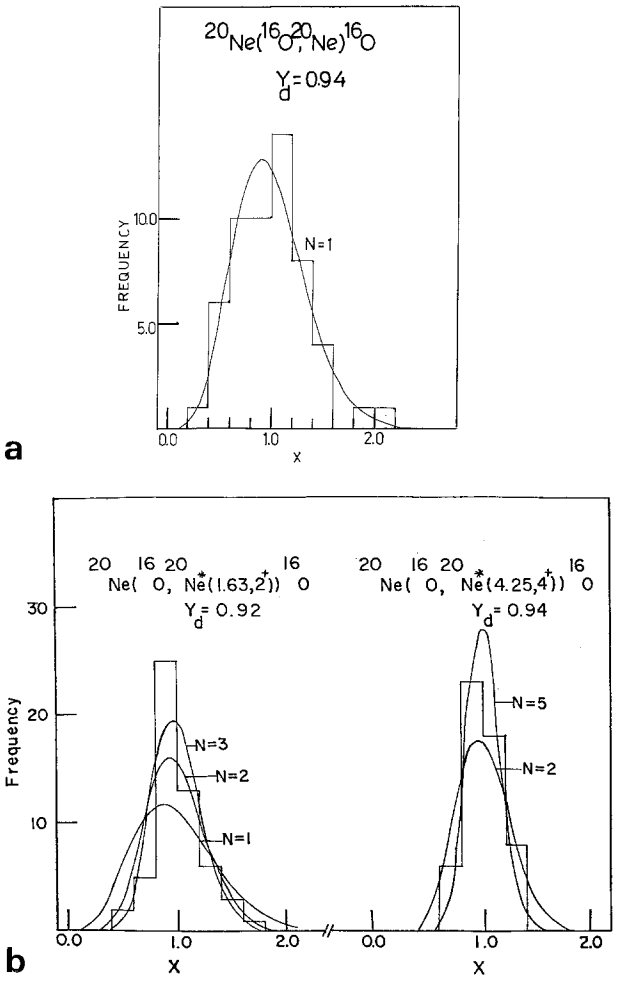

Fig. 6. a Same as in Fig. 4 but for the indicated excitation function of $^{20}Ne(^{16}O, ^{20}Ne)^{16}$ reaction. **b** Same as in Fig. 4 but for the indicated excitation functions of $^{20}Ne(^{16}O, ^{20}Ne)^{16}O$ reaction

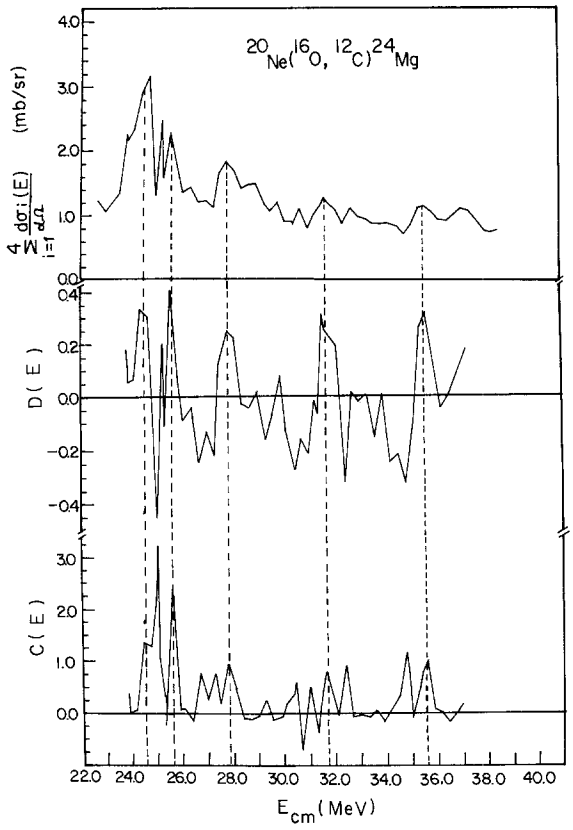

Fig. 7. The Cross-correlation function, $C(E)$ (lower panel), deviation function, $D(E)$ (middle panel) and the summed excitation function $\left(\sum_{i=1}^{4} d\sigma_i(E)/d\Omega\right)$ (upper panel) for $^{20}Ne(^{16}O, ^{12}C)^{24}Mg$ reaction. The vertical dashed lines indicate the locations of the nonstatistical structures

whereas for $^{20}Ne^*(4.25, 4^+)+^{16}O$, the same have been calculated for $N=2$ and $N=5$ (here $N_{max}=5$). The experimental and theoretical distributions of cross sections are compared in Fig. 6b. This comparison also points to large nonstatistical component in the cross sections. In fact the comparison of the experimental and theoretical distributions for the $^{20}Ne^*(1.63, 2^+)+^{16}O$ channel indicates even larger value of Y_d (see Fig. 6b).

2.4. Deviation and Energy Dependent Cross-correlation Functions

For locating the resonant/nonstatistical structures in the excitation functions it is very useful (the correlated structures can be clearly seen) to calculate deviation and energy dependent cross-correlation functions which are respectively defined as [20]

$$D(E)=\frac{1}{M}\sum_{i=1}^{M}\left(\frac{d\sigma_i(E)}{\langle d\sigma_i(E)\rangle}-1\right) \tag{5}$$

$$C(E)=\frac{2}{M(M-1)}\sum_{i>j=1}^{M}\left(\frac{d\sigma_i(E)}{\langle d\sigma_i(E)\rangle}-1\right)\left(\frac{d\sigma_j(E)}{\langle d\sigma_j(E)\rangle}-1\right)\cdot[C_i(0)\,C_j(0)]^{-1/2}. \tag{6}$$

Here $d\sigma_i(E)$ is the differential cross section for the i^{th} excitation function at bombarding energy E, and $\langle\ \rangle$ denotes the corresponding running average taken over the energy interval mentioned earlier. The $C_i(0)$ and $C_j(0)$ are the variances of the i^{th} and j^{th} excitation functions and M is total number of excitation functions. We calculated both these functions for both the reactions. These functions are shown in Fig. 7 for $^{12}C+^{24}Mg$ exit channels. In the same figure we show the summed excitation function $\left(\sum_{i=1}^{4}\frac{d\sigma_i(E)}{d\Omega}\right)$.

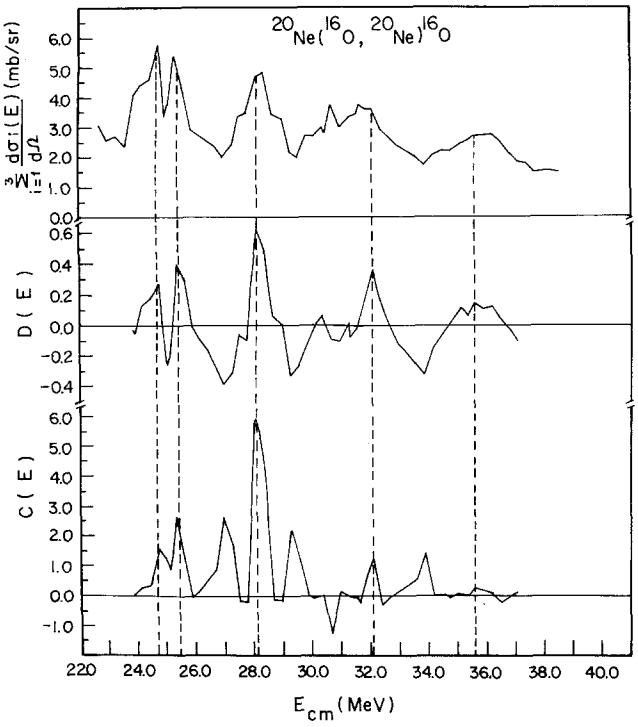

Fig. 8. The same as in Fig. 7 but for the ^{20}Ne(^{16}O, ^{20}Ne)^{16}O reaction

The correlated structures at $E_{c.m.}=24.6$, 25.6, 27.8, 31.7 and 35.5 MeV stand out clearly in all the three functions and qualify to be of nonstatistical origin, specially because the values of $C(E)$ (at corresponding energies) are much larger than $3\sigma_c$ (4.7 to 15.8 times) $\left(\sigma_c=\left[\frac{2}{M(M-1)(n-1)}\right]^{1/2}=0.158,\ n \text{ is the number of data points in the averaging interval, see [22]}\right)$. They are much beyond the statistical limit. For ^{20}Ne(^{16}O, ^{20}Ne)^{16}O reaction the cross-correlation function, deviation function and summed excitation function are shown in Fig. 8. It can be seen that there are correlated structures at $E_{c.m.}=24.7$, 25.4, 28.1, 32.1 and 35.6 MeV. Except for the one at $E_{c.m.}=35.6$ MeV the values of $C(E)$ are much larger (15.4 to 26.5 times) than $3\sigma_c(\sigma_c=0.223)$, the statistical limit. These structures are, therefore, of nonstatistical origin. The indications of the structure at 35.6 MeV are weak ($C(E)=1.12\,\sigma_c$); this structure is corroborated by its prominent appearance in the ^{20}Ne(^{16}O, ^{12}C)^{24}Mg reaction (see Fig. 7). The structure at 25.6 MeV is being reported for the first time. The difference in locations of the correlated structures in the two reactions (see Figs. 7 and 8) might be resulting due to interference effects between background and resonance amplitudes [23]. However, the positions of these resonant/nonstatistical structures are consistent within the quoted energy resolutions ($\sim$0.5 MeV for ^{12}C-channel and $\sim$1.0 MeV for ^{20}Ne-channel) for the measurement of excitation functions.

2.5. *Cross-channel Correlation Coefficients*

According to the standard statistical model [10, 24] there should be no cross correlations between different reaction channels and, therefore, large values of the cross-channel correlation coefficients should be taken as an evidence for the nonstatistical origin of the observed structures in the excitation functions. We calculated the cross-correlation coefficients between different reaction channels by employing the expression [20]

$$C_{ij}=\left\langle\left(\frac{d\sigma_i(E)}{\langle d\sigma_i(E)\rangle}-1\right)\left(\frac{d\sigma_j(E)}{\langle d\sigma_j(E)\rangle}-1\right)\right\rangle \cdot[C_i(0)\,C_j(0)]^{-1/2}. \quad (7)$$

Here subscripts i & j denote the two particular channels in question (and other symbols have been already explained earlier). The cross-channel correlation coefficients thus obtained are given in Table 2. The indicated errors are due to the finite range of data [24]. From this table it can be noted that there are rather large positive correlations between different channels for both the reactions. The large values may specially be noted for g.s.$-(^{12}C+^{24}Mg^*(1.37,\ 2^+))$, $(^{12}C+^{24}Mg^*(1.37, 2^+))-(^{12}C+^{24}Mg^*(6.01, 4^+ +6.43, 0^+))$, $(^{12}C+^{24}Mg^*(4.12,\ 4^+ +4.24,\ 2^+)+^{12}C^*(4.44,\ 2^+)$

Table 2. Cross-channel correlation coefficients for $^{12}C+^{24}Mg$ and $^{20}Ne+^{16}O$ exit channels

Pairs of channels	Correlation coefficient
(a): ^{20}Ne(^{16}O, ^{12}C)^{24}Mg excitation functions	
(g.s.)$-(^{12}C+^{24}Mg^*(1.37, 2^+))$	0.48 ± 0.15
(g.s.)$-[^{12}C+^{24}Mg^*(4.12, 4^+ +4.24, 2^+)$ $+(^{12}C^*(4.44, 2^+)+^{24}Mg)]$	0.32 ± 0.15
(g.s.)$-(^{12}C+^{24}Mg^*(6.01, 4^+ +6.43, 0^+))$	0.35 ± 0.15
$(^{12}C+^{24}Mg^*(1.37, 2^+))$ $-[(^{12}C+^{24}Mg^*(4.12, 4^+ +4.24, 2^+))$ $+(^{12}C^*(4.44, 2^+)+^{24}Mg)]$	0.35 ± 0.11
$(^{12}C+^{24}Mg^*(1.37, 2^+))$ $-(^{12}C+^{24}Mg^*(6.01, 4^+ +6.43, 0^+))$	0.45 ± 0.11
$[(^{12}C+^{24}Mg^*(4.12, 4^+ +4.24, 2^+)$ $+^{12}C^*(4.44, 2^+)+^{24}Mg)]$ $-(^{12}C+^{24}Mg^*(6.01, 4^+ +6.43, 0^+))$	0.61 ± 0.12
(b): ^{20}Ne(^{16}O, ^{20}Ne)^{16}O excitation functions	
g.s.$-(^{20}Ne^*(1.63, 2^+)+^{16}O)$	0.59 ± 0.19
g.s.$-(^{20}Ne^*(4.25, 4^+)+^{16}O)$	0.58 ± 0.15
$(^{20}Ne^*(1.63, 2^+)+^{16}O)-(^{20}Ne^*(4.25, 4^+)+^{16}O)$	0.74 ± 0.11

$+^{24}Mg)-(^{12}C+^{24}Mg^*(6.01, 4^+ +6.43, 0^+))$, and for all the three pairs of $^{20}Ne+^{16}O$ exit channels. Such large values of cross-correlation coefficients clearly point to the non-statistical nature of the observed structures.

2.6. Coherence Widths

The coherence widths (Γ) in ^{36}Ar were obtained by autocorrelation analysis and empirical estimates. The autocorrelation function is given by [25]

$$C(\varepsilon)=\frac{\langle x(E)\cdot x(E+\varepsilon)\rangle}{\langle x(E)\rangle\cdot\langle x(E+\varepsilon)\rangle}-1$$
$$=\frac{C(0)}{(1+\varepsilon^2/\Gamma^2)} \quad (8)$$

Where ε is a variable energy interval and the symbol $\langle\ \rangle$, as usual, denotes the energy average. The autocorrelation functions for all the excitation functions for both $^{12}C+^{24}Mg$ and $^{20}Ne+^{16}O$ channels are given in Figs. 9 and 10 respectively. The extracted values of coherence widths were corrected for finite range of data effects [26] and are listed in Table 3.

The coherence widths were also estimated by using the empirical relation [27]

$$\Gamma=14\exp(-4.69\sqrt{A/Ex})\ \text{MeV}. \quad (9)$$

Where A is the mass and Ex the excitation energy of the compound nucleus in MeV. According to these estimates the Γ-values ranged between 175 and

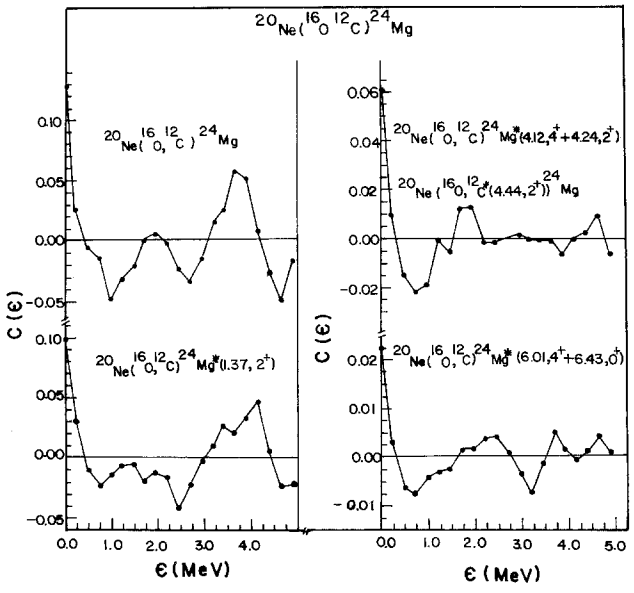

Fig. 9. Autocorrelation functions for $^{20}Ne(^{16}O, ^{12}C)^{24}Mg$ excitation functions

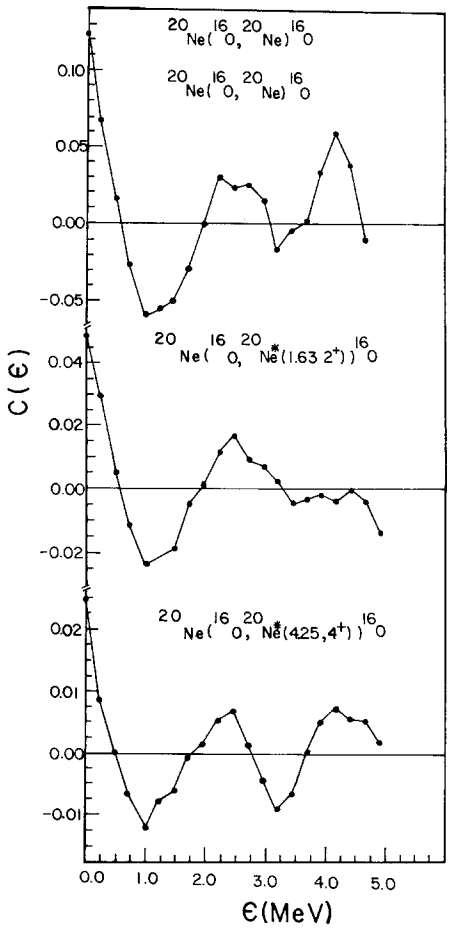

Fig. 10. Same as in Fig. 9, but for $^{20}Ne(^{16}O, ^{20}Ne)^{16}O$ excitation functions

Table 3. Coherence widths obtained from the autocorrelation analysis of all available excitation functions of both the reactions

Excitation Functions (exit-channel)	Γ(keV)
$^{12}C+^{24}Mg$	290±102
$^{12}C+^{24}Mg^*(1.37, 2^+)$	181±51
$^{12}C+^{24}Mg^*(4.12, 4^+ +4.24, 2^+)+^{12}C^*(4.44, 2^+)+^{24}Mg)$	133±32
$^{12}C+^{24}Mg^*(6.01, 4^+ +6.43, 2^+)$	128±31
$^{20}Ne+^{16}O$	262±88
$^{20}Ne^*(1.63, 2^+)+^{16}O$	317±115
$^{20}Ne^*(4.25, 4^+)+^{16}O$	195±57

337 keV in the energy range of excitation functions. These values essentially lie in the same range as obtained by autocorrelation analysis (see Table 3). It may be remarked that noting the relatively poor energy resolution and large energy step size involved in the measurement of the excitation functions it is not justified (because many maxima might be missed) to use the method of counting the maximima to determine the coherence widths from the present data.

3. Conclusion

The deviation functions, energy dependent correlation functions, and the summed excitation functions very clearly exhibit well correlated structures at 24.6, 25.6, 27.8, 31.7 and 35.5 MeV in $^{20}Ne(^{16}O, ^{12}C)^{24}Mg$ and $^{20}Ne(^{16}O, ^{20}Ne)^{16}O$ reactions. High magnitudes (much larger than the statistical limits) of the energy dependent correlation functions at these energies as well as rather large values of cross-channel correlation coefficients very well support the nonstatistical origin of these structures. Hauser-Feshbach cross sections as well as the comparison of experimental and theoretical distributions of cross sections clearly indicate very large nonstatistical component in the cross sections. The Γ-values obtained from autocorrelation analysis lie in the same range as the empirical estimates. The structure at 25.6 MeV is being reported for the first time.

The authors are thankful to the Council of Scientific and Industrial Research, New Delhi for the financial assistance in the form of a Research Scheme. They are grateful to Dr. J. Schimizu for making available the data for this analysis.

References

1. Mermaz, M.C., Greiner, A., Kim, B.T., LeVine, M.J., Mueller, E., Ruscer, M., Petrascu, M., Petrouici, M., Simion, V.: Phys. Rev. C**24**, 1512 (1981)
2. Mermaz, M.C., Greiner, A., LeVine, M.J., Jundt, F., Coffin, J.P., Adoun, A.: Phys. Rev. C**25**, 2815 (1982)
3. Ghosh, B., Singh, R.: Pramana-J. Phys. **29**, 155 (1987)
4. Glaesner, A., Duennweber, W., Hering, W., Konnerth, D., Ritzka, R., Singh, R., Trombik, W.: Phys. Lett. B**169**, 153 (1986)
5. Cindro, N., Moses, J.D., Nelson, S., Cates, M., Drake, D.M., Hanson, D.L., Sunier, J.M.: Phys. Lett. **84**B, 55 (1979)
6. Ford, Jr., J.L.C., Gomez del Campo, J., Shapira, D.: Phys. Lett. **89**B, 48 (1979)
7. Renner, T.R. et al.: Bull. Am. Phys. Soc. **24**, 843 (1979)
8. Schimizu, J., Yokota, W., Nakagawa, T., Fukuchi, Y., Yamaguchi, H., Sato, M., Hanashima, S., Nagashima, Y., Furuno, K., Katori, K., Kubuno, S.: Phys. Lett. **112**B, 323 (1982)
9. Singh, R.: Z. Phys. A – Atoms and Nuclei **311**, 99 (1983)
10. Ericson, T.E.O.: Ann. Phys. (N.Y.) **23**, 390 (1963)
11. Brink, D.M., Stephen, R.O.: Phys. Lett. **5**, 77 (1963)
12. Pappalardo, G.: Phys. Lett. **13**, 320 (1964)
13. Shapira, D., Stokstad, R.G., Bromley, D.A.: Phys. Rev. C**10**, 1063 (1974)
14. Braga Marcazzen, M.G., Milazzo Colli, L.: Prog. Nucl. Phys. **11**, 145 (1970)
15. Stokstad, R.G.: Wright Nuclear Structure Laboratory, Yale University Internal Report No. 52 (1972) (unpublished); the number of effective channels is evaluated by the code STAT2, Stokstad, R.G.: Oak Ridge National Laboratory (unpublished)
16. Hauser, W., Feshbach, H.: Phys. Rev. **87**, 366 (1952)
17. Cramer, J.G.: Heavy Ion optical model code HOP2, University of Washington, Seattle, Report (1974) (unpublished)
18. Singh, R.: North-Eastern Hill University Technical Report No. Phys/Nucl/Rs/2/1988 (unpublished)
19. Dayras, R.A., Stokstad, R.G., Switikowski, Z.E., Wieland, R.M.: Nucl. Phys. A**265**, 153 (1976)
20. Dennis, L.C., Thornton, S.T., Cordell, K.R.: Phys. Rev. C**19**, 777 (1979)
21. Gilfoyle, G.P., Fortune, H.T.: Phys. Rev. C**32**, 865 (1985)
22. Pocanic, D., Caplar, R., Vouruopoulos, G., Aslanoglou, X.: Nucl. Phys. A**444**, 303 (1985)
23. Voit, H., Galster, W., Treu, W., Frohlich, H., Duck, P.: Phys. Lett. **67**B, 397 (1977)
24. Richter, A.: In: Nuclear spectroscopy and reactions. Cerny, J. (ed.), Part C. New York: Academic Press 1974
25. Ericson, T.E.O., Meyer-Kuckuk, T.: Ann. Rev. Nucl. Sci. **16**, 183 (1966)
26. Dallimore, P.G., Hall, I.: Nucl. Phys. **88**, 193 (1966); Halbert, M.L., Durham, F.E., Van der Woude, A.: Phys. Rev. **162**, 899 (1967)
27. Stokstad, R.G.: In: Proceedings of the International Conference on Reactions between Complex Nuclei. Robinson R.L. (ed.), p. 333, Amsterdam: North-Amsterdam: North-Holland 1974

A. Sarma, R. Singh
Physics Department
North-Eastern Hill University
Bijni Complex
Bhagyakul
Shillong 793003
India